NeuroImage 54 (2011) 90–102

Contents lists available at ScienceDirect

NeuroImage

journal homepage: www.elsevier.com/locate/ynimg

Human brain connectivity during single and paired pulse transcranial magnetic stimulation

Florinda Ferreri [a,b,c], Patrizio Pasqualetti [d,e], Sara Määttä [b], David Ponzo [a,c,d], Fabio Ferrarelli [c], Giulio Tononi [c], Esa Mervaala [b], Carlo Miniussi [f,g], Paolo Maria Rossini [a,e,*]

[a] Department of Neurology, University Campus Biomedico, Rome, Italy
[b] Department of Clinical Neurophysiology, Kuopio University Hospital, University of Kuopio, Kuopio, Finland
[c] Department of Psychiatry, University of Wisconsin, Madison WI, USA
[d] AFaR, Department of Neuroscience, Hospital Fatebenefratelli Isola Tiberina, Rome, Italy
[e] IRCCS San Raffaele Pisana e Casa di Cura San Raffaele Cassino, Italy
[f] IRCCS San Giovanni di Dio, Hospital Fatebenefratelli, Brescia, Italy
[g] Department of Biomedical Sciences and Biotechnologies, National Institute of Neuroscience, University of Brescia, Italy

ARTICLE INFO

Article history:
Received 2 June 2010
Accepted 26 July 2010
Available online 1 August 2010

Keywords:
Motor cortex
Cortical effective connectivity
EEG
Navigated transcranial magnetic stimulation
SICI/ICF

ABSTRACT

Objective: Intracortical inhibition (SICI) and facilitation (ICF) in the human motor cortex can be measured using a paired pulse transcranial magnetic stimulation (ppTMS) protocol. Recently, a technical device has been introduced, which allows recording electroencephalographic (EEG) responses to TMS of a given scalp site. The latency, amplitude and scalp topography of such responses are considered a reflection of cortico-cortical connectivity and functional state. The aim of the present study is to better characterize the neuronal circuits underlying motor cortex connectivity as well as the mechanisms regulating its balance between inhibition and facilitation by means of EEG navigated-ppTMS coregistration.
Methods: Sub-threshold and supra-threshold single and ppTMS of the left primary motor cortex were carried out during a multi-channel EEG recording on 8 healthy volunteers; the between-pulse intervals used in the paired pulse trials were 3 (for SICI) and 11 ms (for ICF). Motor evoked potentials (MEPs) from the opposite hand were simultaneously recorded.
Results: Single and ppTMS induced EEG responses characterized by a sequence of negative deflections peaking at approximately 7, 18, 44, 100 and 280 ms alternated with positive peaks at approximately 13, 30, 60 and 190 ms post-TMS. Moreover, ppTMS modulated both EEG evoked activity and MEPs. Amplitude variability of EEG responses was correlated with – and therefore might partially explain – amplitude variability of MEPs.
Interpretation: EEG-ppTMS is a promising tool to better characterize the neuronal circuits underlying cortical effective connectivity as well as the mechanisms regulating the balance between inhibition and facilitation within the human cortices and the corticospinal pathway.

Introduction

Transcranial magnetic stimulation (TMS) is a non-invasive technique that allows the investigation of the functional state of the cerebral cortex. In TMS the excitation of neurons in deep gray matter can be either direct or indirect through volleys from superficial neurons (Barker et al., 1985). Adequate stimulation of the primary motor cortex (M1) evokes indirect excitation of pyramidal neurons via local inter-neurons with higher probability than direct excitation (Amassian and Cracco, 1987). The volley along the corticospinal pathway can elicit electromyographic (EMG) responses, termed motor evoked potentials (MEPs), in the target muscles contra-lateral to the side of the stimulation (Hallett, 2000), thus providing a reliable, *but indirect*, measure of pyramidal tract excitability as well as its cortico-cortical and cortico-subcortical connections. Amplitudes and latencies of MEPs are parameters resulting from a combination of excitatory and inhibitory events occurring in a complex synaptic network at different neural levels along the motor pathway (Ferreri et al 2003; Rossini and Rossi, 2007), although the relative contribution of these events is far from being fully elucidated. Paired pulse TMS techniques (ppTMS; Kujirai et al., 1993) include a well-known paradigm to test this intracortical inhibitory/facilitatory balance by means of a sub-threshold conditioning stimulus (S1) followed by a supra-threshold test stimulus (S2). The test responses are inhibited at inter-stimulus intervals (ISIs) of 1–5 ms and are facilitated at ISIs of 8–30 ms; these phenomena are referred as short intracortical inhibition

* Corresponding author. Dipartimento di Neuroscienze, Università Campus Biomedico di Roma, Via Alvaro del Portillo 21, 00128 Roma. Fax: +39066837360.
E-mail address: paolomaria.rossini@afar.it (P.M. Rossini).

1053-8119/$ – see front matter © 2010 Elsevier Inc. All rights reserved.
doi:10.1016/j.neuroimage.2010.07.056

(SICI) and intracortical facilitation (ICF). The effect of S1 on the size of control MEP is thought to originate at the cortical level (Shimizu et al., 1999; Orth et al., 2003). It is in fact known that a supra-threshold stimulus determines a corticospinal output leading to a MEP, while a sub-threshold stimulus only excites local, cortical inter-neurons (Di Lazzaro et al., 2002). Thus, by combining a sub-threshold pulse with a supra-threshold pulse one can assess the effects of inter-neurons on cortical output (Ziemann et al., 1998). A significant limitation for the understanding of physiological basis of SICI and ICF is that M1 excitatory/inhibitory balance has only been indirectly investigated by means of MEPs amplitude modulation (Ferreri et al., 2006). Recently, a technical device has been introduced that allows recording electro-encephalographic (EEG) responses to TMS of a given scalp site with millisecond resolution. Combining TMS with EEG enables a non-invasive, finally direct, method to study cortical reactivity and connectivity (Ilmoniemi et al., 1997). A network of neuronal connections is in fact engaged when TMS-evoked activation extends from a stimulation site to other parts of the brain and the summation of synaptic potentials produces deflections in scalp EEG signals, starting a few milliseconds after stimulus and lasting about 300 ms, first in the form of rapid oscillations and then as lower-frequency waves (Ilmoniemi and Karhu, 2008). The amplitude, latency, and scalp topography of single pulse TMS-evoked EEG responses have been clearly described (Komssi et al., 2004). The characteristics of these responses are thought to depend on the stimulation intensity and functional state of the stimulated cortex as well as the overall brain. Particularly, it has been suggested that the very first part of the TMS-evoked EEG response reflects the reactivity – that is the functional state – of the stimulated cortex while its spatio-temporal distribution over the scalp reflects the spread of activation to other cortical areas via intra and inter-hemispheric cortico-cortical connections as well as to subcortical structures and spinal cord via projection fibres — that is the effective connectivity of the stimulated area (Lee et al., 2003; Komssi and Kähkönen 2006). The EEG correlates of SICI and ICF as well as their relationships with MEPs modulation have yet to be clearly demonstrated (Daskalakis et al., 2008). In the present study our purposes were, extending previous preliminary results (Paus et al., 2001; Komssi et al., 2004) by means of EEG navigated-ppTMS coregistration, to characterize the neuronal circuits underlying human M1 connectivity, to evaluate SICI and ICF directly from the cortex using EEG and to investigate whether EEG measures of SICI and ICF are related to the same mechanisms underlying EMG measures of SICI and ICF.

Materials and methods

Subjects

Eight healthy young female volunteers (age range, 18–30 years) participated to the protocol during their luteal phase of menstrual cycle to avoid the confounding effect of the ovarian cycle on the motor cortex excitability (Smith et al., 2002). In this way we obtained a homogenous group then some attention should be paid before generalizing our results. A written informed consent was obtained before the experiment, after approval by the Ethics Committee. Subjects were instructed to abstain from caffeine, alcohol, and medication and to maintain their regular sleep–wake schedule on the 3 days before the experimental session. All subjects were right-handed (handedness score 0.70), as evaluated by the Handedness Questionnaire. The exclusion criteria established by international safety standards for TMS were followed (Rossini et al., 1994).

Transcranial magnetic stimulation

Single and paired pulse TMS (biphasic pulse configuration) of the left M1 were performed according with standardized methods (Kujirai et al., 1993; Ziemann et al., 1996), during a multi-channel EEG recording. Two magnetic stimulators were connected to a Bistim device (Magstim Company Limited, Whitland, UK) and to a standard figure-of-eight double 70 mm coil oriented to elicit a posterolateral–anteromedial current flow in the brain. The virtual cathode of the coil was placed over the 'hot spot' of hand area of left M1, defined as the point from which stimuli at the minimal excitability threshold of TMS triggered MEPs of maximal amplitude and minimal latency in the target hand muscle. Then, the resting motor threshold (RMT) was identified according to international guidelines as the stimulator's output able to elicit reproducible MEPs (at least 50 μV in amplitude) in about 50% of 10–20 consecutive stimuli (Rossini et al., 1994). Being this a stereotactic TMS–EEG experiment, the coordinates of the head, the EEG electrodes, and the coil were determined and transformed to the same coordinate system with magnetic resonance (MR) images (Krings et al., 1997). In this way TMS was continuously targeted to the hot spot. Each subject underwent a 1-h session consisting of twelve 5-min blocks, each containing 60 TMS trials. Two supra-threshold single pulse blocks (n 120 trials in total) were randomly intermixed with two 3-ms (n 120 trials in total) and two 11-ms blocks (n 120 trials in total) of paired pulse TMS in order to test SICI and ICF respectively; the intertrial interval was 4–6 s that avoids habituation with repeated stimulation (Kujirai et al., 1993; Sanger et al., 2001; Ziemann et al., 1996). The stimulus intensity for the first *conditioning* pulse (S1) was set at 80% of the RMT and the second *test* pulse (S2) was given supra-threshold with an intensity of 120% of the RMT. Subjects were seated in an armchair with elbows flexed at 90° and prone hands in a relaxed position, eyes open fixed a target over the opposite wall.

Amplitudes of MEPs were measured between the two major and stable peaks of opposite polarity; the amplitude of the conditioned MEPs was expressed as the ratio of the control MEP elicited by the test stimulus alone. Latencies of the MEPs were measured at the maximum positive peak. The elicited compound EMG responses were recorded bilaterally from the first dorsal interosseus muscle (FDI), Ag/AgCl-coated electrodes filled with conductive jelly in a belly/tendon montage. Skin/electrode resistances were below10 KOhm.

EEG recordings

TMS-compatible EEG equipment (BrainAmp 32MRplus, BrainProducts GmbH, Munich, Germany) was used allowing continuous data recording without saturation of the EEG signals and does not require pinning the preamplifier output to a constant level during TMS (Bonato et al., 2006; Veniero et al., 2009). The EEG activity was continuously acquired from 19 scalp sites using electrodes positioned according to the 10–20 International System (Fp1, Fp2, F7, F3, Fz, F4, F8, T3, C3, Cz, C4, T4, T5, P3, Pz, P4, T6, O1, and O2). Additional electrodes were used as ground and reference. The ground electrode was positioned in Oz in order to have maximal distance from the stimulating coil. The linked mastoid served as the reference for all electrodes. The signal was bandpass filtered at 0.1–500 Hz and digitized at a sampling rate of 2.5 kHz. In order to minimize overheating of the electrodes by the stimulating coil, TMS-compatible Ag/AgCl-coated electrodes were used. Skin/electrode impedance was maintained below 5 kOhm. Horizontal and vertical eye movements were detected by recording the electro-oculogram (EOG). The voltage between two electrodes located to the left and right of the external canthi recorded horizontal eye movements. The voltage between reference electrodes and electrodes located beneath the right eye recorded vertical eye movements and blinks. The epochs of the TMS-related scalp EEG responses were selected off-line, started 100 ms before and ended 1000 ms after TMS onset.

Reduction of confounding factors

TMS click and attentional effects

The click associated with the coil's discharge propagates through air and bone and can elicit an auditory N1–P2 complex at latencies of

100–200 ms (Nikouline et al., 1999). To mask coil-generated clicks a white noise, obtained from the waveform of the TMS click digitized and processed to produce a continuous audio signal with its specific time-varying frequencies (Massimini et al., 2005), was continuously delivered through earphones. We adjusted the masking volume until the subjects reported that the TMS click was not audible (always below 90 dB). To ensure wakefulness throughout the recording sessions, subjects were required to keep their eyes open and to fixate on a target over the opposite wall. Additionally (Conte et al., 2008), subject's lapses of attention were controlled with a signal detection task during the experiment (Chee et al., 2008). Brief tones were randomly played through the subject's headphones. These tones were rare compared to the number of TMS pulses delivered (from 3 to 6 tones during each block), and were played at irregular intervals. The subject was instructed to count the tones and report their numbers at the end of the block. At the end of the session the global counting error was always below 5%.

Control experiment

When combining ppTMS with EEG, a possible confound which needs to be accounted for is the effect of the early and late EEG evoked responses to the first pulse (S1) on the early EEG evoked responses to the second pulse (S2). In fact it is known that a single TMS pulse delivered at 80% of MT has a clear effect on the EEG (Komssi et al 2004; Komssi and Kähkönen for review 2006). That is, the EEG evoked responses of the S1 (delivered at 80% of the RMT) may produce a signal sufficient to interfere with the early evoked responses to the S2 (delivered at 120% of the RMT) that may, in part, be responsible for the modulation seen in the EEG signals. In accordance with few studies examining the cortical integration of two consecutive evoked potentials (Foxe et al., 2000; Schürmann et al., 2001; Molholm et al., 2002), it could be argued that cortical excitability modulation occurs if the EEG–TMS responses at ISI 3 or 11 differ from the artificial summed (80% + 120%) waves at that ISI. To control for this, in four subjects we also collected the EEG–TMS responses to S1 alone. We then artificially summed S2 EEG responses shifted by 3 ms and 11 ms to S1 responses once and aligned all signals to the second stimulus (see later). By doing so, artificial EEG–TMS responses were obtained which were statistically compared to these at the real ISIs.

Data analysis

Data analysis was conducted using MATLAB 2008b version 7.7 (MathWorks, Natick, Mass.) and the public license toolbox EEGLAB (Delorme and Makeig, 2004). To compare single trials with paired pulse trials, in the latter all the signals were aligned to S2 by shifting back the traces by 3 or 11 ms respectively. All EEG–TMS-evoked activities were visually inspected in each channel and trials contaminated by environmental noise, muscle activity, or eye movement were rejected together with the corresponding MEPs. Following this procedure, EEG signals were baseline corrected (100 ms prestimulus) and average referenced.

Time domain was the main aspect of the TMS-evoked potentials investigated. To do that, the global-mean field power (GMFP) – a measure of global brain activation calculated as the root mean-squared value of the EEG signal across all electrodes – was first calculated to identify differences in TMS-evoked activity between the conditions (Lehmann and Skrandies, 1980). Then, in each trial and each electrode semi-automatic amplitude/latency measurements of each component of the EEG evoked potentials and corresponding MEP were carried out. We chose not to consider the averaged signals in order to have the best chances to investigate eventual correlations linking TMS-induced EEG deflections and MEPs amplitudes.

Statistical evaluation was conducted by a biostatistician and a computer scientist engineer with expertise in TMS and EEG analysis (P.P and D.P). The dataset suitable for statistical analysis was a matrix constituted by 8 (subjects) × 3 (conditions) × 9 (peaks) × 19 (electrodes) × 120 (stimuli) = 492,480 rows and 2 (EEG: latency and amplitude) + 4 (MEP: latency and amplitudes, contra-lateral and ipsilateral) = 6 columns. In addition, 4 subjects also underwent TMS at 80%, which allowed computing artificial 80% + 120% EEG oscillations to be compared with ISI3 and ISI11 TMS-evoked waves. Therefore, the complete dataset originally comprised 738,720 rows. Then, after cleaning data the available dataset consisted of ~600,000 rows. Besides raw EEG and MEP data, their TMS modulations were computed in the following way. MEP values were log-normally distributed and were therefore log-transformed $y = \log_e(\mathrm{MEP} + 1)$ to achieve a good approximation to gaussianity and to limit the potentially detrimental effect of right-skewed outliers. For each subject i, the average of about 100 single pulse TMS at 120% was computed ($\mathrm{mean}_{i,120\%}$) and percentage variations was obtained from each MEP value according to the formula

$$MEP\_modulation_{i,j,k}\% = 100 * \left[\log_e\left(MEP_{i,j,k} + 1\right) - mean_{i,}120\%\right] / mean_{i,}120\%$$

where

i	subject number, ranging 1–8,
j	TMS condition: 120%, ISI3, ISI11,
k	TMS stimulus, ranging 1–≅100

Similarly, for each subject, each latency peak and each electrode

$$EEG\_modulation_{i,j,l,m,k}\% = 100 * \left[EEG_{i,j,l,m,k} - mean_i, 120\%, l, m\right] / mean_i, 120\%, l, m$$

where

i	subject number, ranging 1–8,
j	TMS condition: 120%, ISI3, ISI11,
k	TMS stimulus, ranging 1–100
l	latency peak, ranging from 1 (N7) to 9 (N280)
m	electrode (1 = Fp1,..., 19 = O2).

To be noted that EEG data were not previously log-transformed since negative values occurred even for “positive” peaks. In order to avoid the influence of outliers, especially for the assessment of MEP–EEG correlations, percentiles were computed for each subject and values below 3rd percentile or above 97th percentile were discarded. After this procedure, the approximately 100 stimuli × 8 subjects = 800 MEP modulations and the 100 stimuli × 8 subjects × 9 peaks × 19 electrodes = 136800 EEG modulations were obtained. The corresponding distributions are represented in Fig. 1, B and D. The distributions of all EEG modulations, regardless to peaks and electrodes, are represented for the three TMS conditions (Fig. 1, B). The distributions are quite symmetric but clearly leptokurtic (values at center and on the tails are more represented than in Gaussian distribution). In MEP data (Fig. 1, D), the typical Gaussian distribution was obtained for single pulse TMS at 120% (confirmed by a very low Kolmogorov–Smirnov statistic = 0.035) and at ISI 11, while a peculiar bimodal distribution was observed ad ISI 3, probably due to a cluster of MEP amplitudes strongly reduced (or even fully suppressed) and to a cluster with of MEP with an partial reduction (never involving the absence of the evoked potential). See result section for a more detailed description of the finding.

As specified in the Introduction, the purpose of statistical analysis was manifold and will be presented in the Result section. However, to link tightly the objectives and the statistical procedure, the following assessments were performed: 1) TMS effects (120%, ISI3 and ISI11) on MEP values (as a confirmation of well-known literature data), 2) TMS

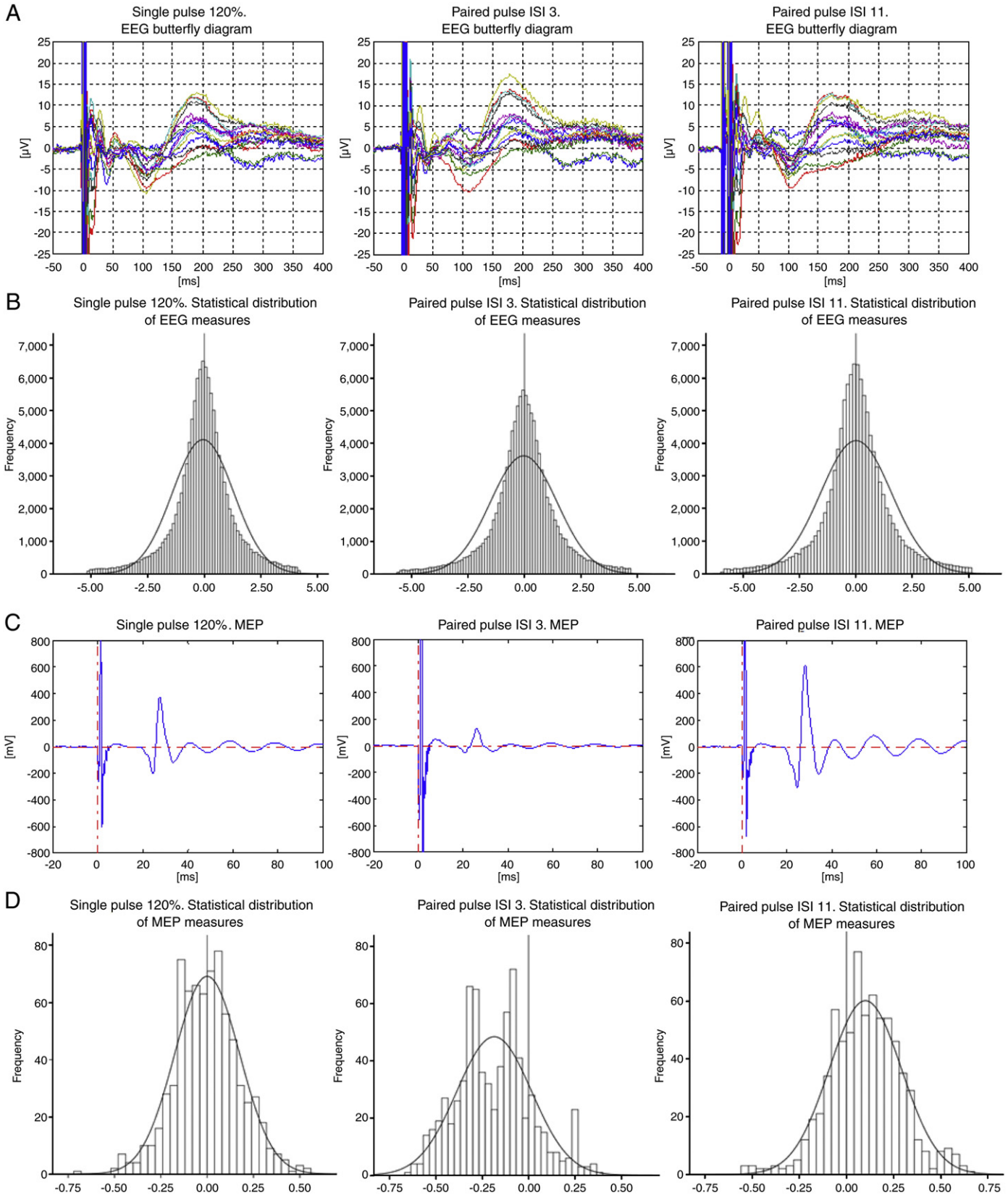

Fig. 1. A: grand average of TMS-evoked potentials recorded at all electrodes in each condition, superimposed in a butterfly diagram. In the pp sessions all signals were aligned to the second stimulus, shifting back the traces by 3 or 11 ms respectively. Polarity of the waveforms is plotted with negative values downward in this and following figures. B: statistical distributions of EEG measures in the experimental conditions. C: grand average of the MEPs in each condition. D: statistical distributions of MEP measures in the experimental conditions.

effects (120%, ISI3 and ISI11) on EEG values, and 3) correlation between EEG modulation and MEP modulation.

To obtain the above assessments, a General Estimating Equation model (hereafter, GEE) was applied with Subject as repeated variable. To take into account the possible autocorrelation of the time series in each subject, the auto-regressive structure was chosen as the working correlation matrix.

The details of each model are the following:

1. GEE with MEP as dependent variable and *Condition* as predictor (factor); Sidak's post-hoc procedure was used to assess the significance of the pair-wise comparisons between the three factor levels (120%, ISI3, ISI11)
2. For each condition (120%, ISI3, ISI11) and peak (N7, P13, N18, P30, N44, P60, N100, P190, and N280), GEE was applied with EEG amplitude as dependent variable and electrode as factors. This procedure allowed to obtain an estimate of the standardized effect size of each peak in each electrode, indicated by a t-statistic (adjusted according to Sidak's procedure). Whenever t-statistic was between −2 and +2, the null hypothesis of peak absence could not be rejected. In addition, the lack of overlapping between Sidak's adjusted 95% confidence intervals was used as conservative procedure to evaluate whether a) a peak was more represented in some areas than in others and b) a peak was modulated by ISI. Despite this procedure which should be able to manage the variability of the EEG maps and to detect reliable average patterns, it is worth noting that single EEG measures in the three experimental conditions presented large portions of overlap. To limit the number of figures the maps of differences between conditions (ISI) were not represented.
3. Possible correlations between EEG (independent) and MEP (dependent) were also initially assessed by means of GEE. However, we observed that such procedure was reliable to address points 1) and 2), but not sufficiently robust to investigate point 3), given the limited number (N = 8) of subjects. Therefore, sample correlation coefficients between EEG and MEP were computed for each subject, peak and electrode, allowing the examination of the repeatability of each correlation across subjects. Before averaging, correlation coefficients were transformed according to Fisher transformation:

$$z = \sqrt{n-3}\frac{1}{2}\log\frac{1+r}{1-r}$$

Results

A. Motor evoked potentials

A.1. Resting motor threshold

In the examined group the threshold values ranged between 50.6 and 56.4% of the maximal stimulator's output.

A.2. ISI and MEP

The characteristic relationship between ISI and MEP ratios was observed (Kujirai et al., 1993; Ziemann et al., 1996; Fig. 1, C). At ISI 3, 83% of MEP was below the mean value at 120% and the corresponding two-modal distribution revealed two peaks of inhibition (Fig. 1, D) due to some subjects with relatively high MEP values at 120% and stronger inhibition at ISI 3 as well to some others with relatively low MEP values at 120% and slighter inhibition at ISI 3. At ISI 11, 71% of MEP was above the mean value at 120%, indicating facilitation (Fig. 1, C and D). To remember that the modulations (percentage variations) of MEP were obtained after log-transformation, thus an inhibition of 20% corresponds roughly to a change from 300 μV to 100 μV and a facilitation of 10% to a change from 300 μV to 530 μV.

According to the output of the General Estimating Equation (from now on called GEE procedure), where MEP was entered as dependent variable (with log. as link function), TMS condition as factor and Subject as repeated variable, TMS modulated significantly MEP (Wald Chi-square = 70.675, df = 1, $p<.001$). The estimated mean values resulted in *578* (95% CI: 307, 848) for supra-threshold single pulse with an intensity of 120% of the RMT, *181* (95% CI: 104, 258) for paired pulse ISI 3 ms and *923* (95% CI: 573, 1274) for paired pulse ISI 11 ms (Fig. 1, C). Each pair-wise comparison was consistently significant ($p<.007$ with Sidak's correction).

B. TMS-evoked EEG responses

As already described (Ilmoniemi et al., 1997; Paus et al., 2001; Komssi et al., 2002, 2004, 2007; Nikulin et al., 2003; Kähkönen et al., 2004, 2005; Kähkönen and Wilenius, 2007; Massimini et al., 2005; Bonato et al., 2006; Daskalakis et al., 2008; Farzan et al., 2009; Lioumis et al. 2009), supra-threshold single pulse TMS of the left MI evoked EEG activity lasting up to 300 ms (for review Komssi and Kähkönen, 2006). In each experimental condition (single and paired pulse TMS, see later) and in each subject, the EEG signals were composed at vertex by a sequence of deflections of negative polarity peaking at approximately 7, 18, 44, 100, and 280 ms alternated with positive polarity peaks at approximately 13, 30, 60 and 190 ms post-TMS, as illustrated in Figs. 1A and 2A. In Fig. 2, B the GMFP in the three experimental conditions is shown.

B.1. Supra-threshold single pulse TMS-evoked activity.

GEE allowed to identify specific EEG pattern on the scalp in each peak (Table 1).

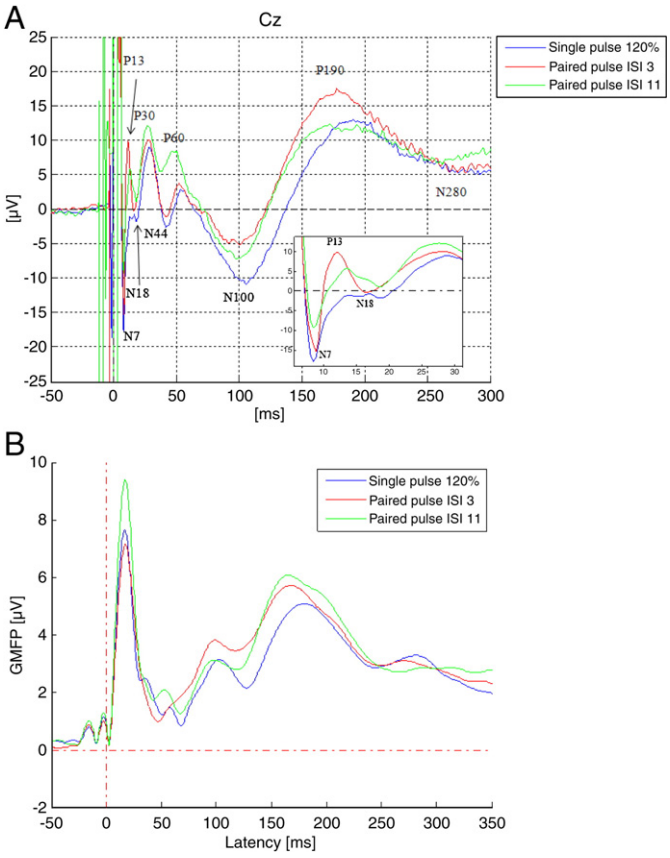

Fig. 2. A: grand average of the EEG responses recorded at vertex (Cz) in supra-threshold single pulse stimulation as well as ISI 3 and ISI 11 paired pulse stimulations. In paired pulse sessions all the signals were aligned to the second supra-threshold stimulus, shifting back the traces by 3 or 11 ms respectively. B: total activation produced by single and paired pulse TMS over the left M1 as measured by the GMF.

N7 (mean latency = 7.1; SD = 2.5) was observed in F3, in the stimulated hemisphere (Fig. 3, A).

P13 (mean latency = 13.1; SD = 2.8) was mainly localized in the contra-lateral hemisphere in (Fp2, F4, F8, C4, T4 and T6. Fig. 3, B).

N18 (mean latency = 18.4; SD = 3.5) was localized in the posterior areas of the stimulated site, strongest in P3 (Fig. 3, C).

P30 (mean latency = 28.8; SD = 5.3) was found in almost each electrode of the nonstimulated hemisphere as well as in Cz, Pz, and T3 (Fig. 4, A).

N44 (mean latency = 44.1; SD = 5.8) showed a diffuse spatial distribution, with an antero-posterior amplitude gradient, being the posterior mean amplitude of about 20% more than the anterior values (Fig. 4, B).

P60 (mean latency = 62.6; SD = 9.5) was observed posteriorly and contra-lateral to the stimulation site. Specifically, the largest amplitude was observed in T5, right behind the stimulation site (Fig. 4, C).

N100 (mean latency = 103.3; SD = 19.3) largest amplitude was observed in C3, the stimulation site with an antero-posterior gradient (Fig. 5, A).

P190 (mean latency = 189.7; SD = 24.3) showed the highest activation in the centro-parietal region of nonstimulated hemisphere (C4, P4; Fig. 5, B).

N280 (mean latency = 266.7; SD = 32.2) showed a diffuse spatial distribution, even if its amplitude was particularly large in correspondence to F3–C3 (Fig. 5, C).

B.2. ISI 3 and ISI 11. ISI 3 and ISI 11 versus supra-threshold single pulse. ISI 11 versus ISI 3

The general EEG patterns observed after ppTMS at ISI 3 as well as ISI 11 are substantially similar to that observed after single pulse (Table 1). However, GEE allowed to identify specific modulations in each peak.

N7 at ISI 3 (mean latency = 7.1, SD = 2.5) was localized, as in supra-threshold single pulse TMS, only in F3. At ISI 11 (mean latency = 7.2, SD = 2.8) was not statistically evident anywhere (Fig. 3, A). The subtraction of different maps showed in F3 slight non-significant difference between single pulse and ISI 11 as well as between ISI 11 and ISI 3 ($p > .05$).

P13 both at ISI 3 (mean latency = 12.8, SD = 2.3) and at ISI 11 (mean latency = 12.6, SD = 3.1) had the same spatial localization as in supra-threshold single pulse, being statistically evident in the region of contra-lateral hemisphere and generally more represented at ISI 3 (Fig. 3, B). The subtraction of different maps confirmed higher amplitudes at ISI 3 versus single pulse in F4 (Sidak's $p = .032$) and at ISI 11 versus single pulse in F4 (Sidak's $p = .041$) and in F8 (Sidak's $p = .043$).

N18 had a different spatial localization at ISI 3 (mean latency = 18.7, SD = 2.1) with respect to ISI 11 (mean latency = 17.6, SD = 3.1) and to single pulse, extending from the posterior regions of the stimulated hemisphere to the more anterior ones (Fig. 3, C). However, the subtraction of different maps showed no clearly significant difference of this peak ($p > .05$).

P30 had at ISI 3 (mean latency = 28.4, SD = 5.1) and at ISI 11 (mean latency = 26.5, SD = 5.3) almost the same spatial localization than in supra-threshold single pulse and was attenuated at ISI 3 and generally stronger at ISI 11 (Paus et al., 2001, Fig. 4, A) in the not stimulated hemisphere. However, the subtraction of different maps showed no clearly significant difference of this peak ($p > .05$).

N44 was spatially modulated by the paired pulse stimulations being virtually absent in the contra-lateral hemisphere at ISI 11 (mean latency = 43.5, SD = 5.3) (Fig. 4, B). The subtraction of different maps confirmed clear differences between ISI 11 and supra-threshold single pulse (Paus et al., 2001) in the contra-lateral hemisphere, mostly in the posterior regions (P4: Sidak's $p = .035$; Pz: Sidak's $p = .042$) and

Table 1
Values are means ± SD; ▲ wave slightly stronger with respect to single pulse; ▲▲ wave stronger with respect to single pulse; ▼ wave attenuated with respect to single pulse; ▼▼ wave cancelled with respect to single pulse; ▼▼▼ wave reversed in polarity with respect to single pulse; — wave stable with respect to single pulse; ○, +, − respectively no correlation, positive and negative EEG–MEP correlation.

		Single pulse	ISI 3	ISI 11
N7	Electrodes	F3	▲F3	▼▼
	Latency	7.1 ± 2.5	7.1 ± 2.5	7.2 ± 2.8
	EEG-MEPc	○	○	○
P13	Electrodes	Fp2,F4,F8,C4,T4,T6	▲▲Fp2,F4,F8,C4,T4,T6	▲Fp2,F4,F8,C4, T4, T6
	Latency	13.1 ± 2.8	12.8 ± 2.3	12.6 ± 3.1
	EEG-MEPc	○	○	+ Fp2,F4,Fz,F8
N18	Electrodes	P3	▲P3,C3,F3	—P3
	Latency	18.4 ± 3.5	18.7, SD = 2.1	17.6, SD = 3.1
	EEG-MEPc	○	○	○
P30	Electrodes	Fp1,Fp2,Fz,F4,F8,Cz,C4, T4,Pz,P4,T6,O1,O2	▼Fp1,Fp2,Fz,F4,F8,Cz, C4,T4,Pz,P4,T6,O1, O2	▲Fp1,Fp2,Fz,F4,F8,Cz, C4,T4,Pz,P4,T6,O1,O2
	Latency	28.8 ± 5.3	28.4 ± 5.1	26.5 ± 5.3
	EEG-MEPc	+ C4,T4,Pz, P4,O2	○	+ F4
N44	Electrodes	Fp1,Fp2,F7,F3,Fz,F4,F8,T3, C3,Cz,C4,T4,T5,P3,Pz,P4, T6,O1,O2	▲F3,C3,P3, ▼Fz,Pz,Cz	▲F3,C3,P3, ▼▼ Fz,F4,Cz,C4,T4, T5,P3,Pz,P4,T6
	Latency	44.1 ± 5.8	43.5 ± 5.3	40.7 ± 5.6
	EEG-MEPc	−F3,T3,C3,Cz,T5,Pz,O1	−T3,T5,01	○
P60	Electrodes	C3, T5, P3, Pz,O1,O2	▼▼▼C3 — T5, P3, Pz,O1,O2	—C3, T5, P3, Pz, O1, O2 ▲ Cz
	Latency	62.6 ± 9.5	62.8 ± 9.4	59.2 ± 9.6
	EEG-MEPc	○	○	○
N100	Electrodes	Fp1,Fp2,F7,F3,Fz,F4,F8, T3,C3,Cz,C4,T4,T5,P3,Pz, P4,T6,O1,O2	▲C3	▲ C3
	Latency	103.3 ± 19.3	102.6 ± 19.1	99.9 ± 16.4
	EEG-MEPc	○	○	○
P190	Electrodes	Fp1,Fp2,F7,F3,Fz,F4,F8, T3,C3,Cz,C4,T4,T5,P3,Pz, P4,T6,O1,O2	▼▼ C3 ▲ F8,Cz,C4,Pz	▼▼ C3 — F8, Cz, C4, Pz
	Latency	189.7 ± 24.3	185.1 ± 24.1	177.6 ± 25.6
	EEG-MEPc	○	○	○
N280	Electrodes	Fp1,Fp2,F7,F3,Fz,F4,F8, T3,C3,Cz,C4,T4,T5,P3,Pz, P4,T6,O1,O2	▲ Fp1,Fp2, F7,F3,Fz, F4,F8,T3,C3,Cz,C4,T4, T5,P3,Pz,P4,T6,O1,O2	▲ Fp1,Fp2,F7,F3,Fz, F4,F8,T3,C3,Cz,C4,T4, T5,P3,Pz,P4,T6,O1,O2
	Latency	266.7 ± 32.2	269.3 ± 32.0	271.9 ± 33.0
	EEG-MEPc	○	○	○

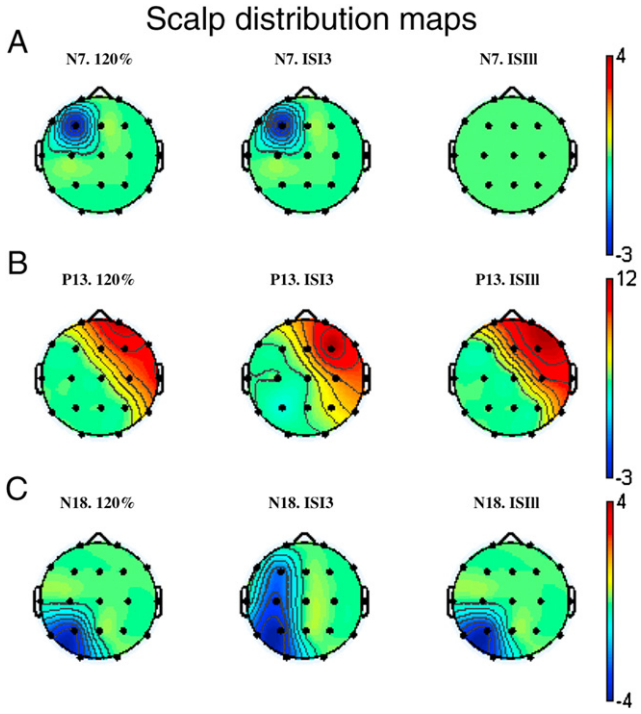

Fig. 3. Scalp distribution maps of General Estimating Equation model EEG pattern at 7, 13 and 18 ms after single and paired pulse stimulation over the left M1. Topographic head plots of cortical evoked activity were obtained by EEGLAB toolbox (Delorme and Makeig, 2004). A: *N7* was localized in F3 after supra-threshold single pulse TMS and ISI 3, after ISI 11 was not statistically evident anywhere. B: in each experimental condition *P13* was statistically evident in the anterior regions of contra-lateral hemisphere and generally stronger at ISI 3. C: *N18* was localized in P3 after supra-threshold single pulse TMS and ISI 11 and had a different spatial localization at ISI 3, extending from the posterior regions of the stimulated hemisphere to the more anterior ones.

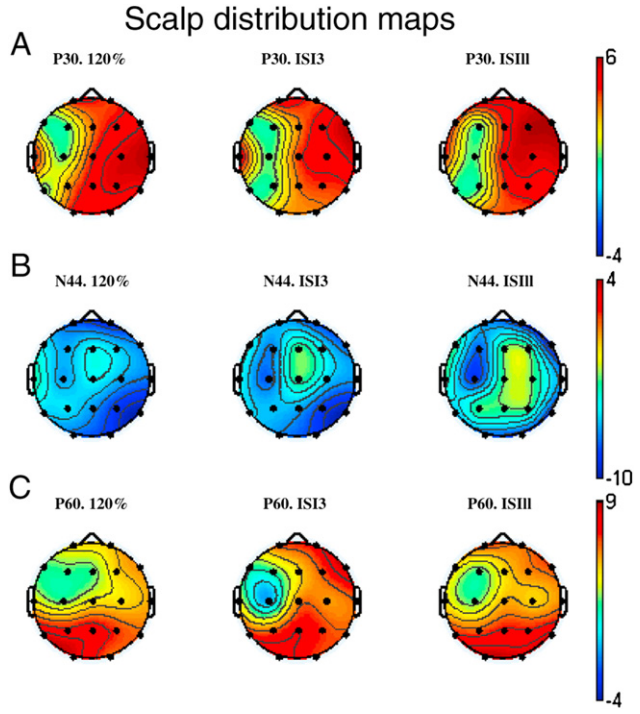

Fig. 4. Scalp distribution maps of General Estimating Equation model EEG pattern at 7, 13 and 18 ms after single and paired pulse stimulation over the left M1. Topographic head plots of cortical evoked activity were obtained by EEGLAB toolbox (Delorme and Makeig, 2004). A: *P30* had almost the same spatial localization in each experimental condition, being attenuated at ISI 3 and generally stronger at ISI 11 in the not stimulated hemisphere. B: *N44* peak showed a diffuse spatial distribution, with an antero-posterior amplitude gradient. It was spatially modulated by the paired pulse stimulations being slightly stronger in C3, P3 and F3 at ISI 3 and virtually absent in the contra-lateral hemisphere at ISI 11. C: *P60* was found posterior and contra-lateral to the stimulation site and was modulated by the ppTMS being the polarity of the peak virtually inverted at ISI 3 in the stimulated area. At ISI 11 it was generally stronger in Cz and in the contra-lateral hemisphere.

between ISI 11 and ISI 3 (mean latency = 40.7, SD = 5.6) in the same areas (P4: Sidak's p = .039; Pz: Sidak's p = .047).

P60 was also found to be modulated by the paired pulse stimulations being the polarity of the peak virtually inverted at ISI 3 (mean latency = 62.8, SD = 9.4) in the stimulated area (Fig. 4, C). At ISI 11 (mean latency = 59.2, SD = 9.6) it was generally stronger in Cz and in the contra-lateral hemisphere. The subtraction of different maps confirmed in C3 clear differences between ISI 3 and supra-threshold single pulse (Sidak's p = .011) as well as between ISI 3 and ISI 11 (Sidak's p = .015).

N100 was found all over the scalp being more topographically represented after ISI 3 (mean latency = 102.6, SD = 19.1) and ISI 11 (mean latency = 99.9, SD = 16.4) than in supra-threshold single pulse on the stimulated area (Fig. 5, A). The subtraction of different maps showed significant differences in the stimulated area (C3) between ISI 3 and the supra-threshold single pulse (Sidak's p = .044) as well as between ISI 11 and the supra-threshold single pulse (Sidak's p = .045).

Also *P190* (Fig. 5, B) was found all over the scalp but in the stimulated area where it was virtually absent after ISI 3 (mean latency = 185.1, SD = 24.1) and ISI 11 (mean latency = 177.6, SD = 25.6). The subtraction of different maps did not indicate specific areas with significant differences among the three conditions.

Finally, *N280* was found all over the scalp and was generally stronger at ISI 3 (latency mean = 269.3, SD = 32.0) and 11 (latency mean = 271.9, SD = 33.0) than in supra-threshold single pulse but at T3 (Fig. 5, C). The subtraction of different maps confirmed the differences between ISI 3 and supra-threshold single pulse and ISI 11 and supra-threshold single pulse in the stimulated area (C3:Sidak's p = .039 and p = .049, respectively).

B.3. Latencies modulation

As a whole, latency was prolonged at ISI 3 of about 2% (2.1; 95% CI = 1.9–2.2) and shortened at ISI 11 (Paus et al., 2001) of about 4% (4.4; 95% CI = 4.3–4.5) (for a paradigmatic channel see Fig. 2, A). Significant latency modulation ($p<0.01$) was consistently observed in each of the nine considered peaks.

N7 latency slightly but significantly (Sidak's p = .007) increased at ISI 3 versus 120%. No other pair-wise difference. The effect size of such modulation was minimal (0.13 ms).

At *P13*, latency decreased after paired pulse stimulations versus 120% (ISI 3 p = 0.012 and ISI 11 p < .001) and was longer at ISI 3 than at ISI 11 (p = 0.011; less than 0.5 ms).

N18 was slightly prolonged at ISI 3 versus 120% (p = .041), shortened at ISI 11 versus 120% (p < .001) and obviously more shortened at ISI 11 versus ISI 3 (p < .001; about 1 ms).

P30 latency decreased after paired pulse stimulations (ISI 3 versus 120%, p < .001, ISI11 versus 120% p < .001) and again at ISI 11 was found the minimal latency. In this case, the maximal difference (between ISI 11 and 120%) was around 2.2 ms.

A similar pattern was observed at *N44*, with each pair-wise comparison significant (p < .001). The maximal difference, corresponding to a decrease of 3.9 ms was between ISI 11 and 120%.

P60 did not change between ISI 3 and 120% (p = 0.999) and strongly decreased at ISI 11 (p < .001) of about 4.5 ms (for a paradigmatic channel see Fig. 2, A).

N100 showed a different pattern with respect to *P60*, since the two paired pulse produced very close latencies (p = .999), clearly shorter than 120% (p < .001) of about 3.9 ms.

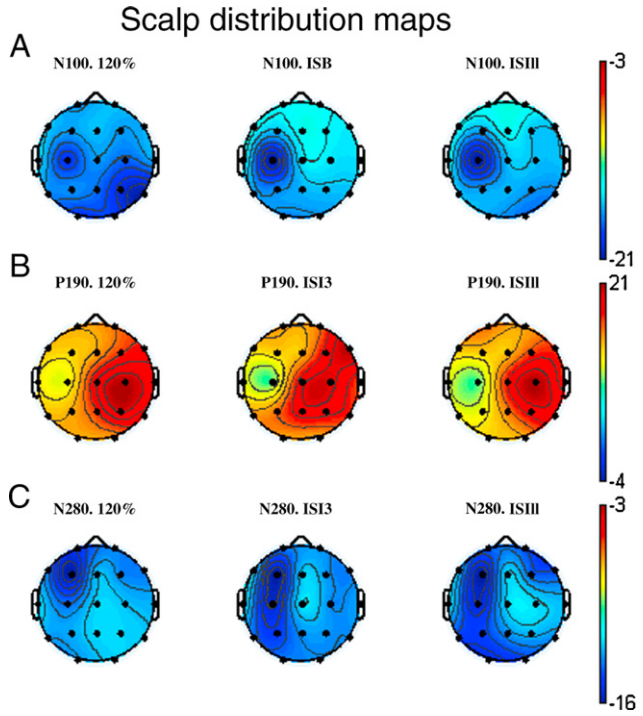

Fig. 5. Scalp distribution maps of General Estimating Equation model EEG pattern at 7, 13 and 18 ms after single and paired pulse stimulation over the left M1. Topographic head plots of cortical evoked activity were obtained by EEGLAB toolbox (Delorme and Makeig, 2004). A: *N100* largest amplitude was observed in C3 stronger after the ppTMS stimulation. B: *P190* was found all over the scalp but in the stimulated area where it was virtually absent after ISI 3. C: *N280* was found all over the scalp and was generally stronger at ISI 3 and 11 than in supra-threshold single pulse but at T3.

P190 was shortest at ISI 11 ($p<.001$ versus both other conditions) and longer at 120% versus ISI 3.

Finally, *N280* did not change between ISI 3 and 120% ($p=0.999$) and between ISI 11 and 120% ($p=0.887$).

C. Correlation between EMG and EEG measures

The correlation between EEG, considered as the independent variable, and MEPs, considered as dependent variable, was statistically significant for some of the peaks considered. More precisely, in order to reduce the total number of possible correlations, we report here only correlations corresponding to peaks that showed significant changes across conditions. In addition, to take into account the problem of multiple comparisons, a correlation was considered significant only when its 95% Sidak's confidence intervals did not include the reference value corresponding to null hypothesis ($r=0$, or equivalently $z=0$, being $z=\sqrt{n-3}\frac{1}{2}\log\frac{1+r}{1-r}$).

Particularly, for *P13* there were no clear correlations with the MEPs' amplitude after the single pulse TMS and paired pulse TMS at ISI 3; however after ppTMS at ISI 11 a positive correlation was seen in F8 and F4 with a slight involvement of Fp2 and Fz (Fig. 6, B).

At *P30* a positive correlation with the MEPs amplitude after the single pulse TMS was observed in the non stimulated hemisphere. No correlation with the MEPs amplitude was observed after ppTMS at ISI 3, while at ISI 11 the main finding was the positive correlation between EEG modulation in F4 and MEP modulation (Fig. 7, B).

At *N44* a negative correlation with the MEPs amplitude after the single pulse TMS was observed in the central and posterior regions of the stimulated hemisphere. After paired pulse TMS at ISI 3 the correlation was markedly attenuated, surviving only at T5, T3 and O1. After ISI 11 no clear correlation was observed (Fig. 8, B).

D. EEG control experiment (four subjects)

In the subgroup of four subjects in which we also performed two sub-threshold (80% of the RMT) single pulse blocks (n 120 trials in total) collecting the EEG responses, the peaks' amplitude was found to depend on stimulation intensity (approximately, the mean EEG amplitude at 80% was 40% less than that at 120%). That is, evoked waves were characterized by the same peaks described previously but with a clear amplitude modulation, and their scalp spatial distribution was the same both in sub and in supra-threshold stimulations (Komssi et al., 2004). Peak latencies were prolonged of about 5% at 80% with respect to 120% (4.7; 95% CI = 4.5–4.9). Moreover, as the summed waves at ISI 3 significantly differ from real waves at that ISI as well the summed waves at ISI 11 differ from real waves at that ISI; particularly, the amplitude of artificially summed waves at ISI 3 was approximately 23% higher than real waves at ISI 3 ($p<.001$) and the amplitude of artificially summed waves at ISI 11 was approximately 17% higher than real waves at ISI 11 ($p<.001$). This suggests, in accordance with few studies examining the cortical integration of two evoked potentials (Foxe et al., 2000; Schürmann et al., 2001; Molholm et al., 2002), a clear cortical excitability modulation induced by the paired pulse stimulation.

Discussion

This study adds new insight into previously delineated (Komssi et al., 2004) functional behaviour of human brain as investigated by EEG oscillations evoked by TMS on M1. In fact, two further early responses – N7 and P13 – previously described by some of us (Bonato et al., 2006) were observed and characterized in more details. Moreover, this study confirmed that ppTMS can modulate early and late EEG evoked responses as well as MEPs (Paus et al 2001). This suggests that for some TMS-induced EEG peaks the measures of SICI and ICF are somewhat related to the same mechanisms mediating EMG measures of SICI and ICF. Additionally, it implies that intracortical inhibition and facilitation, which until now could only be indirectly demonstrated in the M1 by measuring MEP amplitude modulation, could be directly evaluated virtually in each cortical area by measuring EEG brain responses to ppTMS (Daskalakis et al., 2008). TMS-evoked brain responses are generated by the temporal and spatial summation in the superficial cortical layers of the electrical currents caused by the slow postsynaptic excitatory (EPSP) and/or inhibitory potentials (IPSP) with little or even no contribution by the brief action potentials. On the other hand, MEP is produced from brief, indirect-induced descending action potentials originated by the activation of pyramidal neurones via pre-synaptic IPSP and/or EPSP (Rossini et al., 1994). This activation follows a combination of intrinsic proprieties of corticospinal tract and inhibitory–excitatory circuit interactions in different proportions depending on the timing, on the stimulus intensity/synchronicity and direction of induced current. However the exact sequence of central pathways and mechanisms involved is not well understood (for details see Ziemann and Rothwell 2000). Moreover, in accordance with intracortical recordings and computerized models, one should also keep in mind that critical events triggering a MEP are thought to happen in the stimulated M1 within the first 5 ms after the TMS (for details see Esser et al., 2005) and should be practically invisible in EEG–TMS recordings, being masked by the magnetic artefact. Anyway, since SICI and ICF are thought to represent separate intracortical phenomena (Ziemann et al. 1996), starting from the 5th millisecond a significant amount of data about the M1 connectivity and functional state can be collected. Particularly, the nearly similar potential patterns elicited by different TMS intensities and paradigm (i.e. single and paired pulse) suggest that a similar sequence of neuronal events is independently triggered for each peak and possibly the same cortical and subcortical circuits are recruited in a pattern of functional connectivity (Lee et al., 2003).

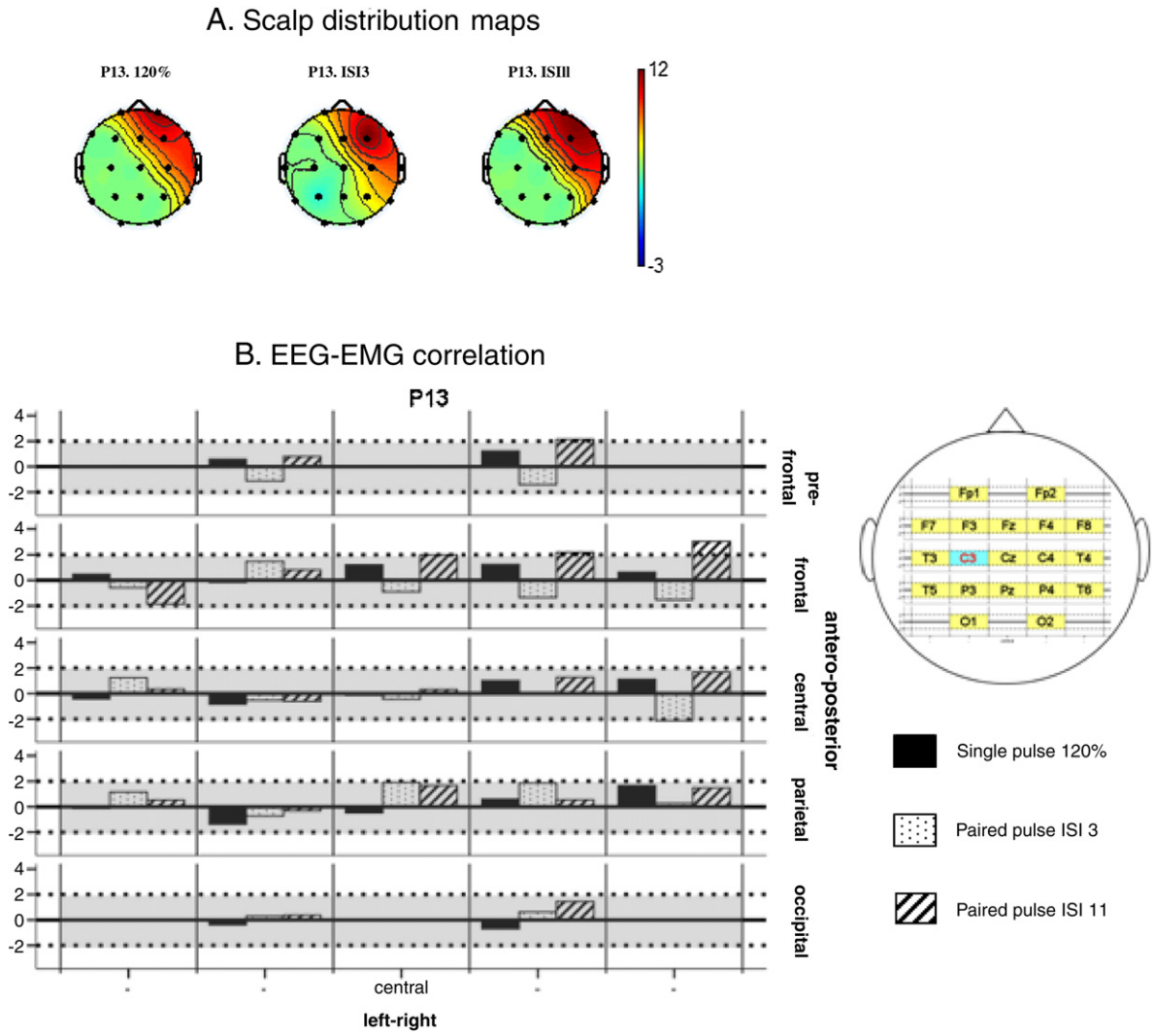

Fig. 6. A: scalp distribution maps of GEE model EEG pattern at 13 ms after stimulation over the left M1. In each experimental condition *P13* was statistically evident in the anterior regions of contra-lateral hemisphere and generally stronger at ISI 3 B: positive correlation after ISI 11 was seen in F8 and F4 with a slight involvement of Fp2 and Fz.

On the other hand, the clear modulation of the amplitude of the evoked peaks as well as of GMFP by different TMS intensities and paradigms provides information about the regulation of functional state of M1 and large-scale connected networks, via different interneuronal circuit activations and/or modulations (Ilmoniemi and Karhu 2008). Then it is reasonable to propose that the EEG–TMS-evoked activity should not be seen as the result of single process and the conventionally negative or positive peaks should not be considered reflecting inhibitory or excitatory circuits net activities but likely a balance of both, as suggested by this experiment where a modulation of the peaks amplitude was often seen at ISI 3 as well at ISI 11 even in the same direction.

Possible molecular origin of the EEG–TMS-evoked responses. Insight into M1 functional state from the ppTMS experiment

The firing of cortical neurons enveloped in the EEG signal is associated to the activation of both fast and slow excitatory postsynaptic potentials (fEPSPs and sEPSPs respectively) as well as fast and slow inhibitory postsynaptic potentials (fIPSPs and sIPSPs, respectively; Rosenthal et al., 1967). Particularly fEPSPs are mediated by non-NMDA, AMPA/kainate receptors with a rise time of 0.5–1.9 ms, being their influence on the TMS-evoked EEG responses probably obscured by the timing of the artefact. On the other hand, sEPSPs are mediated by N-methyl-D-aspartate (NMDA) receptors with a rise times of 4–9 ms, being possibly involved in the generation and/or modulation of N7, while fIPSPs are mediated by GABA**A** postsynaptic receptors lasting approximately 20–30 ms (Davies et al., 1990; Deisz, 1999) and being possibly involved in the generation and/or modulation of P13, N18, P30 and N44. Finally sIPSPs are related to pre-synaptic and postsynaptic GABA**B** receptors with an inhibition that peaks around 100–200 ms starting around 50 ms and lasting up to a few hundred milliseconds, being possibly involved in the P60, N100, P180 and N280 genesis (Tamás et al., 2003; McDonnell et al., 2006).

On this basis SICI as evaluated by means of MEPs amplitude modulation at ISI 3 (Fisher et al., 2002) is thought to explore the net effect of the activation of inhibitory GABA**A** circuits in M1. This activation occurs through the summation at the pyramidal neurons, of pre-synaptic low-threshold GABA**A** fIPSPs elicited by the sub-threshold TMS pulse as well as high-threshold non-NMDA fEPSPs elicited by the supra-threshold pulse. This means that SICI produces MEP inhibition by reducing the late indirect waves (Hanajima et al., 1998; Di Lazzaro et al., 2002), and that in the EEG evoked activity should be hidden these hyperpolarizing currents and their 20–30 ms lasting effects on the initial waveform evoked: effectively a modulation at ISI 3 is observable at P13 and slightly at N18 and P30. About the modulations seen afterwards from P60 pass through N100, P180 and N280 waves, their time course could be related to the activity of GABA**B** receptors although their

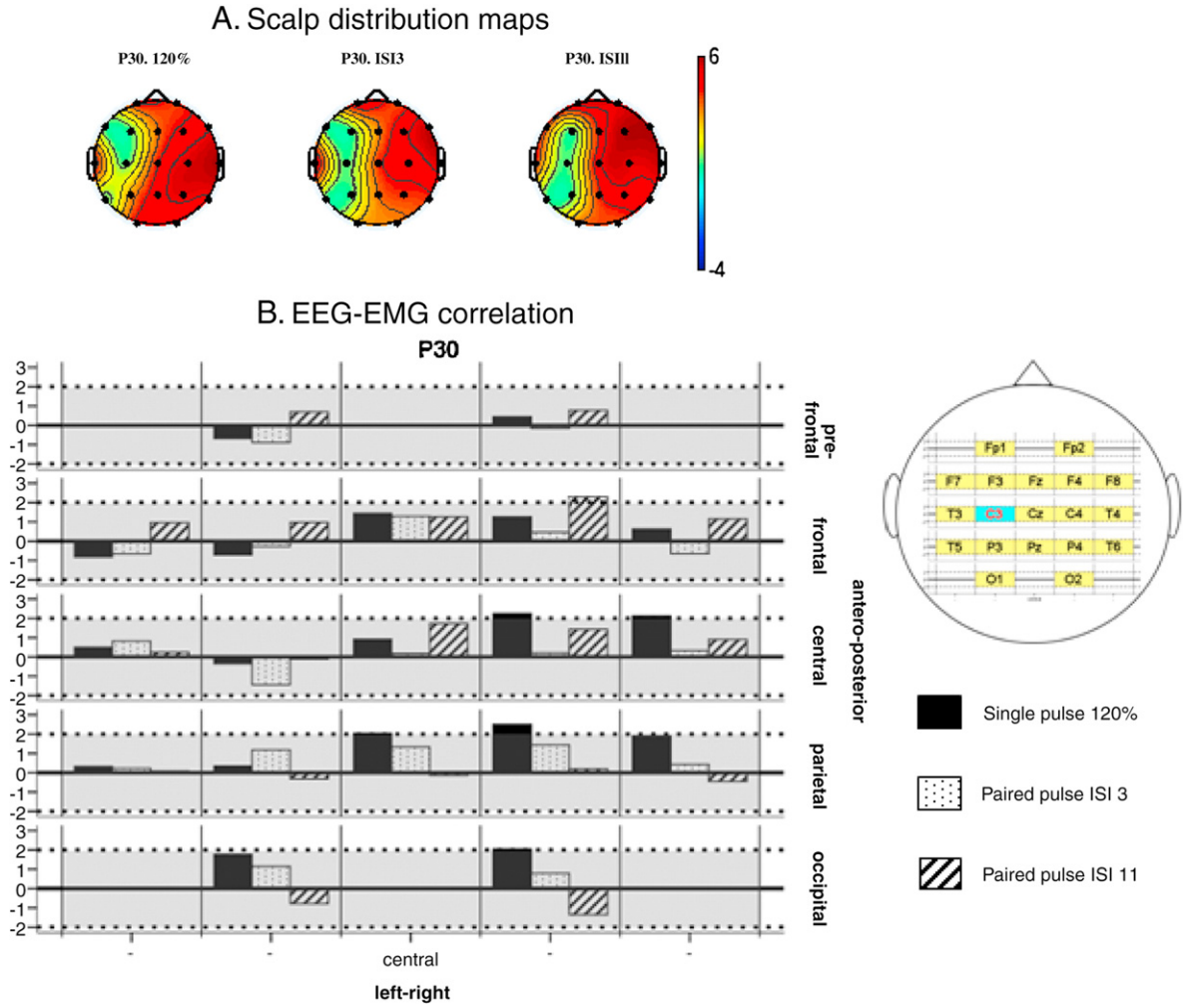

Fig. 7. A: scalp distribution maps of GEE model EEG pattern at 30 ms after stimulation over the left M1. *P30* had almost the same spatial localization in each experimental condition, being attenuated at ISI 3 and generally stronger at ISI 11 in the not stimulated hemisphere. B: positive correlation with the MEPs amplitude after the single pulse TMS was observed in the non stimulated hemisphere. No correlation was observed at ISI 3, while at ISI 11 a positive correlation was found in F4.

activation in SICI is not clearly known. Regarding ICF there is consensus for a cortical (rather than spinal) site of action of the sub-threshold pulse, although emerging data suggest complex mechanisms (Di Lazzaro et al., 2002, 2006). Converging evidence support the idea that ICF can interact with inhibitory circuits and is the result of a net facilitation consisting of prevailing facilitation and weaker inhibition. The inhibition probably comes from GABA**A** fIPSP, the facilitation from NMDA 4–9 ms rising time sEPSP (Ziemann, 2003). Indeed according to this study a modulation at ISI 11 is clearly observable at N7. Moreover in line with previous results we found a clear modulation of N44 (and slightly at P30) at ISI 11. It has been suggested (Paus et al., 2001) that this modulation is related to a disruption of the rhythmic activity of an ongoing M1 pacemaker, which is selectively induced by ISI 11 ppTMS and strictly correlated with beta and gamma oscillatory activity in M1 (Van Der Werf and Paus 2006). Notably, generation of gamma oscillations, as ICF, has been associated, to both GABA**A** and NMDA receptor activities. Regarding the modulation of later waves in respect to supra-threshold single pulse, it seems to reflect quite exactly as to what is seen at ISI 3, suggesting also here an involvement of GABA**B** receptors' activity.

M1 connectivity as evaluated by means of spatial distribution of the EEG–TMS-evoked activity. EEG–MEP modulation correlations

It has been suggested that TMS on M1 predominantly affects the site of stimulation, although according to an emerging principle of reciprocality (Matsumoto et al., 2007) it is known that M1 receives input from, and projects output bilaterally to primary motor, supplementary motor, somatosensory cortices as well as to the thalamus. Recent fMRI and PET studies which however suffer from a poor temporal resolution (for review see Bestmann et al., 2008) have demonstrated some spread of activation from M1 to remote brain areas. Inferring from the existing literature and following M1 anatomical connectivity, we extended previous findings about the physiology of EEG–TMS responses.

The scalp topography of the first wave detected, that is *N7*, suggests the engagement of the ipsilateral non-primary motor cortices, possibly with the prevalent involvement of the premotor one. This could reflect activation extending from the stimulated M1 via cortico-cortical projections, which are modulated by the experimental conditions, being the peak slightly strengthened at ISI 3 and statistically not evident at ISI 11 (Fig. 3, A; for scalp–brain anatomical details see Civardi et al., 2001). Animal data suggested strong connections from primary and non-primary motor cortices, both facilitatory and inhibitory with a predominance of the inhibitory ones at rest. Indeed recent studies (Davare et al., 2008) revealed the clear existence of functional interactions between motor and premotor areas in humans at similar latencies (6–8 ms), although indirectly by means of conditioning ppTMS study.

Wave *P13* (Fig. 3, B), shows clear engagement of the contra-lateral cortices, possibly with the prevalent involvement of the non-primary motor ones, in all the experimental conditions with the strongest

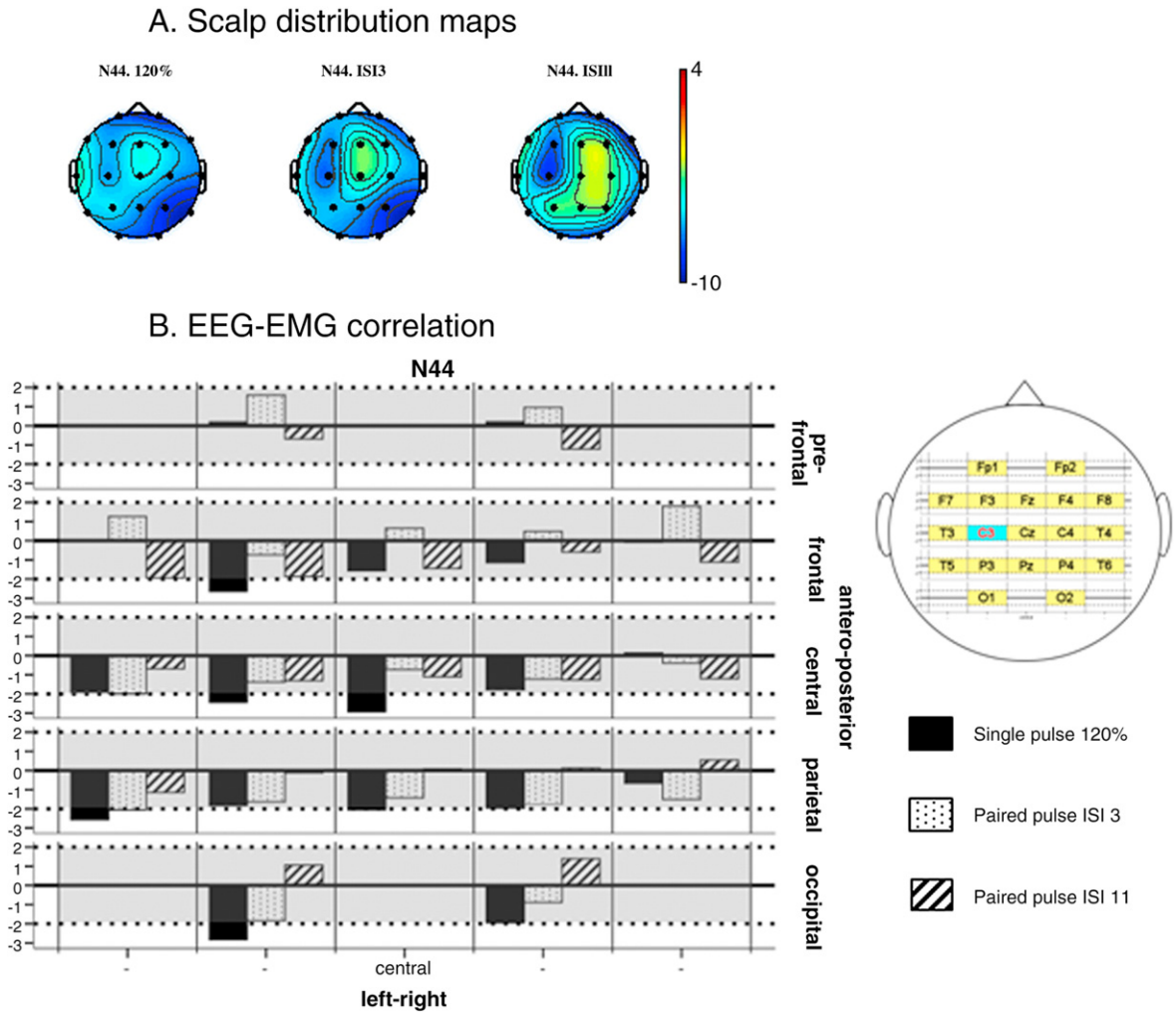

Fig. 8. A: scalp distribution maps of GEE model EEG pattern at 44 ms after stimulation over the left M1. *N44* peak showed a diffuse spatial distribution, with an antero-posterior amplitude gradient. It was spatially modulated by the paired pulse stimulations being slightly stronger in C3, P3 and F3 at ISI 3 and virtually absent in the contra-lateral hemisphere at ISI 11. B: negative correlation after the single pulse TMS was observed in the central and posterior regions of the stimulated hemisphere. After ISI 3 the correlation was markedly attenuated, surviving only at T5, T3 and O1. After ISI 11 no clear correlation was observed.

evidences at ISI 3. This is consistent with the trans-callosal conduction time of 12–15 ms found both in studies using electrical stimulation and TMS (Ferbert et al., 1992; Meyer et al 1998). It was demonstrated that trans-callosal projections are mainly excitatory, synapsing onto local inhibitory circuits mediating SICI and LICI within the target hemisphere (Daskalakis et al., 2002). There have been fewer studies of the inter-hemispheric functional connections between M1 and contra-lateral non-primary motor cortices, despite dense anatomical long-range connections known to exist in animals. Recently, homologous connections and their preferential inhibitory effects were indirectly observed in humans at latencies consistent with our results (10 ms, Mochizuki et al., 2004). The correlation observed with the MEPs amplitude after ISI 11 suggests an involvement of this peak and these cortices in modulating EMG measures of ICF (Fig. 6, B); moreover, if P13 modulation is related to fIPSPs it could be inferred that at this latency the contra-lateral ICF could be mediated by GABA**A** receptors.

Wave *N18* (Fig. 3, C) appears as a focal negativity in P3 (that possibly corresponds to the ipsilateral posterior parietal cortex PPC, Civardi et al., 2001), and could reflect sustained and reverberant activation extending from the stimulated M1 via cortico-cortical projections. Pioneering studies (Meynert, 1865) revealed that PPC is anatomically interconnected with motor, premotor, and more frontal areas through distinct white matter tracts forming the superior longitudinal fasciculus (SLF). Indeed, the existence of functional interactions between the PPC and the ipsilateral M1 was recently revealed (Koch et al., 2007) at a consistent timing (about 15 ms) although indirectly by means of conditioning ppTMS study. Moreover, it was proposed that also parieto-premotor projections, which are known to be more numerous than direct parieto-motor ones transferring information for visuomotor plan and transformations, could be involved in this pathway and modulated by SICI mechanism.

Previous study suggested a complex source structure for the wave *P30* (Van Der Werf et al., 2006), that in this current experiment appears as a strong activation of the contra-lateral hemisphere, which is slightly increased at ISI 11 (Fig. 4, A). This might be expression of a further inter-hemispheric spread of activation via the corpus callosum or a subcortical pathway (via thalamic nuclei and/or basal ganglia) projecting back diffusely to the cortex or both. The thalamus is in fact believed to play a minor role in the generation of early EEG responses to TMS but could be involved in reverberating circuits at longer post-stimulus latencies also explaining the large scalp distribution of the waves seen from now on (Ziemann and Rothwell 2000). The correlation observed with the MEPs amplitude both after single pulse and ISI 11 in contra-lateral hemisphere suggests an involvement of this peak and these brain structures in determining M1 net output and modulating EMG measures of ICF (Fig. 7, B); moreover, if P30 modulation is related to fIPSPs it could be inferred that at this latency the contra-lateral ICF could be mediated by GABA**A** receptors.

Wave *N44* ms was widely distributed with clear spatial and amplitude modulation induced by the experimental conditions (Fig. 4, B). It shows high amplitude in the stimulated area in each condition, while in the parieto-posterior regions of the non stimulated hemisphere it was observed at supra-threshold single pulse and at ISI 3, whereas it was virtually absent at ISI 11. Although it was previously proposed that N44 and MEP should be considered separate markers of functional properties of M1, considering that N44 can arise upon sub-threshold TMS (Van Der Werf and Paus 2006), in this study the correlation of the N44 amplitude in the stimulated hemisphere with the MEP amplitude both after single pulse and ISI 3 suggests a role of this peak and these brain structures in determining M1 net output and modulating EMG measures of SICI (Fig. 8, B); moreover, if N44 modulation is related to fIPSPs it could be inferred that at this latency the SICI could be mediated by GABA**A** receptors. N44 was related to somatosensory evoked potentials generated as feed-back from the TMS-induced muscles twitch; this view is contradicted by the fact that the same component, in some brain areas even stronger than during supra-threshold single pulse session, was also recorded during ISI 3 session (Figs. 4, B and 8 A and B) despite remarkably depressed MEP.

Wave *P60* ms shows a widely distribution with clear spatial and amplitude modulation induced by the experimental conditions (Fig. 4, C). Interestingly enough, this wave is in fact virtually absent in the stimulated area after supra-threshold single pulse TMS and ISI 11 and specifically reversed in polarity at ISI 3.

Wave *N100*, considered the dominant peak in TMS-evoked EEG activity, shows a consistent lateralization on the stimulated side, being stronger both after ISI 3 and 11 than after supra-threshold single pulse TMS (Fig. 5, A). In preliminary experiments it has been connected with a brain response to the coil 'click' and to bone-conducted sound, although later studies have partially excluded such a contamination (Nikouline et al., 1999; Bender et al., 2005; Kicic et al., 2008), suggesting that this component reflects, at least in part, TMS-induced cortical inhibitory process.

The topography of *P190* ms shows a clear and circumscribed involvement of contra-lateral hemisphere without strong modulation by experimental conditions (Fig. 5, B). This component, like N100, has been associated with the auditory N1–P2 complex in previous studies (latency 100–200 ms, Bonato et al., 2006). However, the lateralization found in the current study in the hemisphere opposite to the stimulation and the audio-masking procedure adopted, does not support this hypothesis. Instead its long latency and wide distribution could suggest the engagement of a reverberant cortico-subcortical circuit.

Finally, wave *N280* peaked in the premotor areas of the stimulated hemisphere. A modulation by experimental condition was found both at ISI 3 and 11 with a possible engagement of M1 (Fig. 5, C). As for P190 its long latency and wide distribution could suggest the involvement of a reverberant cortico-subcortical circuit.

Conclusion

It is hereby demonstrated that EEG-ppTMS is a promising tool to characterize the neuronal circuits underlying human cortical effective connectivity as well as the neural mechanisms regulating the balance between inhibition and facilitation within the cortices and the corticospinal pathway. It was in fact proved that ppTMS modulates MEPs as well as EEG early and late evoked responses and that for some peaks the EEG variability is partly linked with – and therefore might partially explain – MEPs' variability. Future studies parsing EEG measures of SICI and ICF into their component frequencies are needed to further characterize their physiology. Several animal studies, computer simulations and finally a human study (Farzan et al., 2009), implicated closely Glutamatergic and GABAergic neurotransmission in both the generation and modulation of theta, beta and gamma frequencies oscillations in the cortex (Amzica and Steriade 1995; Traub et al, 1998; Mann and Paulsen, 2007). Finally, it should be stressed that the correlations observed in this study between EEG and EMG measures do not necessarily imply that the mechanisms subtending EEG responses modulation in the central nervous system are causally linked with those subtending MEPs modulations in SICI and ICF. On the other hand, it is likely that future studies using Glutammate, GABA**A**, as well as GABA**B** receptor agonist or antagonist in healthy subjects would be able to ascertain this relationship more directly.

Acknowledgments

The research was granted by University Campus Biomedico of Rome, Telecom Italia Mobile and Lottomatica.

We gratefully thank Mimma Veniero, Mariella Gurzì and Claudia Fracassi for the help in the data acquiring, Reto Huber, Steve Esser, Brady Reidner and Filippo Zappasodi for their fruitful comments.

This study is in memory of Lorenzo Gatto, MD.

References

Amassian, V.E., Cracco, R.Q., 1987. Human cerebral cortical responses to contralateral transcranial magnetic stimulation. Neurosurgery 20, 148–155.
Amzica, F., Steriade, M., 1995. Short- and long-range neuronal synchronization of the slow (<1 Hz) cortical oscillation. J. Neurophysiol. 73 (1), 20–38.
Barker, A.T., Jalinous, R., Freeston, I.L., 1985. Non-invasive magnetic stimulation of human motor cortex. Lancet 1, 1106–1107.
Bender, S., Basseler, K., Sebastian, I., Resch, F., Kammer, T., Oelkers-Ax, R., Weisbrod, M., 2005. Electroencephalographic response to transcranial magnetic stimulation in children: evidence for giant inhibitory potentials. Ann. Neurol. 58 (1), 58–67.
Bestmann, S., Ruff, C.C., Blankenburg, F., Weiskopf, N., Driver, J., Rothwell, J.C., 2008. Mapping causal interregional influences with concurrent TMS-fMRI. Exp. Brain Res. 191 (4), 383–402 Review.
Bonato, C., Miniussi, C., Rossini, P.M., 2006. Transcranial magnetic stimulation and cortical evoked potentials: a TMS/EEG co-registration study. Clin. Neurophysiol. 117 (8), 1699–1707.
Chee, M.W., Tan, J.C., Zheng, H., Parimal, S., Weissman, D.H., Zagorodnov, V., Dinges, D.F., 2008. Lapsing during sleep deprivation is associated with distributed changes in brain activation. Neurosci. 21 (28(21)), 5519–5528.
Civardi, C., Cantello, R., Asselman, P., Rothwell, J.C., 2001. Transcranial magnetic stimulation can be used to test connections to primary motor areas from frontal and medial cortex in humans. Neuroimage 14, 1444–1453.
Conte, A., Belvisi, D., Iezzi, E., Mari, F., Inghilleri, M., Berardelli, A., 2008. Effects of attention on inhibitory and facilitatory phenomena elicited by paired-pulse transcranial magnetic stimulation in healthy subjects. Exp. Brain Res. 186 (3), 393–399.
Daskalakis, Z.J., Christensen, B.K., Fitzgerald, P.B., Roshan, L., Chen, R., 2002. The mechanisms of interhemispheric inhibition in the human motor cortex. J. Physiol. 15 (543(Pt 1)), 317–326.
Daskalakis, Z.J., Farzan, F., Barr, M.S., Maller, J.J., Chen, R., Fitzgerald, P.B., 2008. Long-interval cortical inhibition from the dorsolateral prefrontal cortex: a TMS–EEG study. Neuropsychopharmacology 33 (12), 2860–2869.
Davare, M., Lemon, R., Olivier, E., 2008. Selective modulation of interactions between ventral premotor cortex and primary motor cortex during precision grasping in humans. J. Physiol. 586 (Pt 11), 2735–2742.
Davies, C.H., Davies, S.N., Collingridge, G.L., 1990. Paired-pulse depression of monosynaptic GABA-mediated inhibitory postsynaptic responses in rat hippocampus. J. Physiol. 424, 513–531.
Deisz, R.A., 1999. GABA(B) receptor-mediated effects in human and rat neocortical neurones in vitro. Neuropharmacology 38 (11), 1755–1766.
Delorme, A., Makeig, S., 2004. EEGLAB: an open source toolbox for analysis of single-trial EEG dynamics including independent component analysis. J. Neurosci. Methods 134, 9–21.
Di Lazzaro, V., Oliviero, A., Mazzone, P., Pilato, F., Saturno, E., Insola, A., Visocchi, M., Colosimo, C., Tonali, P.A., Rothwell, J.C., 2002. Direct demonstration of long latency cortico-cortical inhibition in normal subjects and in a patient with vascular parkinsonism. Clin. Neurophysiol. 113, 1673–1679.
Di Lazzaro, V., Pilato, F., Oliviero, A., Dileone, M., Saturno, E., Mazzone, P., Insola, A., Profice, P., Ranieri, F., Capone, F., Tonali, P.A., Rothwell, J.C., 2006. Origin of facilitation of motor-evoked potentials after paired magnetic stimulation: direct recording of epidural activity in conscious humans. J. Neurophysiol. 96 (4), 1765–1771.
Esser, S.K., Hill, S.L., Tononi, G., 2005. Modeling the effects of transcranial magnetic stimulation on cortical circuits. J. Neurophysiol. 94 (1), 622–639.
Farzan, F., Barr, M.S., Wong, W., Chen, R., Fitzgerald, P.B., Daskalakis, Z.J., 2009. Suppression of gamma oscillations in the dorsolateral prefrontal cortex following long interval cortical inhibition: a TMS–EEG study. Neuropsychopharmacology 34 (6), 1543–1551.

Ferreri, F., Pauri, F., Pasqualetti, P., Fini, R., Dal Forno, G., Rossini, P.M., 2003. Motor cortex excitability in Alzheimer's disease: a transcranial magnetic stimulation study. Ann. Neurol. 53, 102–108.
Ferreri, F., Curcio, G., Pasqualetti, P., De Gennaro, L., Fini, R., Rossini, P.M., 2006. Mobile phone emissions and human brain excitability. Ann. Neurol. 60 (2), 188–196.
Ferbert, A., Priori, A., Rothwell, J.C., Day, B.L., Colebatch, J.G., Marsden, C.D., 1992. Interhemispheric inhibition of the human motor cortex. J. Physiol. 453, 525–546.
Fisher, R.J., Nakamura, Y., Bestmann, S., Rothwell, J.C., Bostock, H., 2002. Two phases of intracortical inhibition revealed by transcranial magnetic threshold tracking. Exp. Brain Res. 143 (2), 240–248.
Foxe, J.J., Morocz, I.A., Higgins, B.A., Murray, M.M., Javitt, D.C., Schroeder, C.E., 2000. Multisensory auditory–somatosensory interactions in early cortical processing revealed by high density electrical mapping. Cogn. Brain Res. 10, 77–83.
Hallett, M., 2000. Transcranial magnetic stimulation and the human brain. Nature 13 (406(6792)), 147–150 Jul. Review.
Hanajima, R., Ugawa, Y., Terao, Y., Sakai, K., Furubayashi, T., Machii, K., Kanazawa, I., 1998. Paired-pulse magnetic stimulation of the human motor cortex: differences among I waves. J. Physiol. 1 (509(Pt 2)), 607–618.
Ilmoniemi, R.J., Virtanen, J., Ruohonen, J., Karhu, J., Aronen, H.J., Näätänen, R., Katila, T., 1997. Neuronal responses to magnetic stimulation reveal cortical reactivity and connectivity. NeuroReport 8, 3537–3540.
Ilmoniemi, R.J., Karhu, J., 2008. TMS and electroencephalography: methods and current advances. In: Wassermann, E., Epstein, C., Ziemann, U., Walsh, V., Paus, T., Lisanby, S. (Eds.), In the Oxford Handbook of Transcranial Stimulation. Oxford University Press, pp. 593–608.
Kähkönen, S., Wilenius, J., Komssi, S., Ilmoniemi, R.J., 2004. Distinct differences in cortical reactivity of motor and prefrontal cortices to magnetic stimulation. Clin. Neurophysiol. 115 (3), 583–588.
Kähkönen, S., Komssi, S., Wilenius, J., Ilmoniemi, R.J., 2005. Prefrontal transcranial magnetic stimulation produces intensity-dependent EEG responses in humans. Neuroimage 24, 955–960.
Kähkönen, S., Wilenius, J., 2007. Effects of alcohol on TMS-evoked N100 responses. J. Neurosci. Methods 166, 104–108.
Kicic, D., Lioumis, P., Ilmoniemi, R.J., Nikulin, V.V., 2008. Bilateral changes in excitability of sensorimotor cortices during unilateral movement: combined electroencephalographic and transcranial magnetic stimulation study. Neuroscience 152, 1119–1129.
Koch, G., Fernandez Del Olmo, M., Cheeran, B., Ruge, D., Schippling, S., Caltagirone, C., Rothwell, J.C., 2007. Focal stimulation of the posterior parietal cortex increases the excitability of the ipsilateral motor cortex. J. Neurosci. 20 (27(25)), 6815–6822.
Komssi, S., Aronen, H.J., Huttunen, J., Kesaniemi, M., Soinne, L., Nikouline, V.V., Ollikainen, M., Roine, R.O., Karhu, J., Savolainen, S., Ilmoniemi, R.J., 2002. Ipsi- and contralateral EEG reactions to transcranial magnetic stimulation. Clin. Neurophysiol. 113, 175–184.
Komssi, S., Kähkönen, S., Ilmoniemi, R.J., 2004. The effect of stimulus intensity on brain responses evoked by transcranial magnetic stimulation. Hum. Brain Mapp. 21, 154–164.
Komssi, S., Kähkönen, S., 2006. The novelty value of the combined use of electroencephalography and transcranial magnetic stimulation for neuroscience research. Brain Res. Rev. 30 (52(1)), 183–192 Review.
Komssi, S., Savolainen, P., Heiskala, J., Kähkönen, S., 2007. Excitation threshold of the motor cortex estimated with transcranial magnetic stimulation electroencephalography. NeuroReport 18, 13–16.
Krings, T., Buchbinder, B.R., Butler, W.E., Chiappa, K.H., Jiang, H.J., Rosen, B.R., Cosgrove, G.R., 1997. Stereotactic transcranial magnetic stimulation: correlation with direct electrical cortical stimulation. Neurosurgery 41 (6), 1319–1325.
Kujirai, T., Caramia, M.D., Rothwell, J.C., Day, B.L., Thompson, P.D., Ferbert, A., Wroe, S., Asselman, P., Marsden, C.D., 1993. Corticocortical inhibition in human motor cortex. J. Physiol. 471, 501–519.
Lee, L., Harrison, L.M., Mechelli, A., 2003. A report of the functional connectivity workshop, Dusseldorf. Neuroimage 19 (2 Pt 1), 457–465.
Lehmann, W., Skrandies, D., 1980. Reference-free identification of components of checkerboard-evoked multichannel potential fields. Electroencephalogr. Clin. Neurophysiol. 48 (6), 609–621.
Lioumis, P., Kičić, D., Savolainen, P., Mäkelä, J.P., Kähkönen, S., 2009. Reproducibility of TMS-Evoked EEG responses. Hum. Brain Mapp. 30 (4), 1387–1396.
Mann, E.O., Paulsen, O., 2007. Role of GABAergic inhibition in hippocampal network oscillations. Trends Neurosci. 30, 343–349.
Massimini, M., Ferrarelli, F., Huber, R., Esser, S.K., Singh, H., Tononi, G., 2005. Breakdown of cortical effective connectivity during sleep. Science 309, 2228–2232.
Matsumoto, R., Nair, D.R., LaPresto, E., Bingaman, W., Shibasaki, H., Lüders, H.O., 2007. Functional connectivity in human cortical motor system: a cortico-cortical evoked potential study. Brain 130 (Pt 1), 181–197.
McDonnell, M.N., Orekhov, Y., Ziemann, U., 2006. The role of GABA(B) receptors in intracortical inhibition in the human motor cortex. Exp. Brain Res. 173 (1), 86–93.
Meyer, B.U., Röricht, S., Woiciechowsky, C., 1998. Topography of fibres in the human corpus callosum mediating interhemispheric inhibition between the motor cortices. Ann. Neurol. 4, 360–369.
Meynert, 1865. Anatomie der hirnrinde und ihre verbindungsbahnen mit den empfindenden oberflachen und den bewegenden massen. Leidesdorf's lehrbuch der phychischen krankheiten. Germany.
Mochizuki, H., Huang, Y.Z., Rothwell, J.C., 2004. Interhemispheric interaction between human dorsal premotor and contralateral primary motor cortex. J. Physiol. 15 (561 (Pt 1)), 331–338.
Molholm, S., Ritter, W., Murray, M.M., Javitt, D.C., Schroeder, C.E., Foxe, J.J., 2002. Multisensory auditory–visual interactions during early sensory processing in humans: a high-density electrical mapping study. Brain Res. Cogn. Brain Res. 14 (1), 115–128.
Nikouline, V., Ruohonen, J., Ilmoniemi, R.J., 1999. The role of the coil click in TMS assessed with simultaneous EEG. Clin. Neurophysiol. 110 (8), 1325–1328.
Nikulin, V.V., Kicić, D., Kähkönen, S., Ilmoniemi, R.J., 2003. Modulation of electroencephalographic responses to transcranial magnetic stimulation: evidence for changes in cortical excitability related to movement. Eur. J. Neurosci. 18 (5), 1206–1212.
Orth, M., Snijders, A.H., Rothwell, J.C., 2003. The variability of intracortical inhibition and facilitation. Clin. Neurophysiol. 114, 2362–2369.
Paus, T., Sipilä, P.K., Strafella, A.P., 2001. Synchronization of neuronal activity in the human primary motor cortex by transcranial magnetic stimulation: an EEG study. J. Neurophysiol. 86, 1983–1990.
Rosenthal, J., Waller, H.J., Amassian, V.E., 1967. An analysis of the activation of motor cortical neurons by surface stimulation. J. Neurophysiol. 30 (4), 844–858.
Rossini, P.M., Barker, A.T., Berardelli, A., Caramia, M.D., Caruso, G., et al., 1994. Non-invasive electrical and magnetic stimulation of the brain, spinal cord and roots: basic principles and procedures for routine clinical application. Electroencephalogr. Clin. Neurophysiol. 91, 79–92.
Rossini, P.M., Rossi, S., 2007. Transcranial magnetic stimulation: diagnostic, therapeutic, and research potential. Neurology 13 (68(7)), 484–488 Review.
Sanger, T.D., Garg, R.R., Chen, R., 2001. Interactions between two different inhibitory systems in the human motor cortex. J. Physiol. 530.2, 307–317.
Shimizu, T., Oliveri, M., Filippi, M.M., Palmieri, M.G., Pasqualetti, P., Rossini, P.M., 1999. Effect of paired transcranial magnetic stimulation on the cortical silent period. Brain Res. 834, 74–82.
Schürmann, M., Nikouline, V.V., Soljanlahti, S., Ollikainen, M., Basar, E., Ilmoniemi, R.J., 2001. EEG responses to combined somatosensory and transcranial magnetic stimulation. Clin. Neurophysiol. 112 (1), 19–24.
Smith, M.J., Adams, L.F., Schmidt, P.J., Schmidt, P.J., Rubinow, D.R., Wassermann, E.M., 2002. Effects of ovarian hormones on human cortical excitability. Ann. Neurol. 51, 599–603.
Tamás, G., Lorincz, A., Simon, A., Szabadics, J., 2003. Identified sources and targets of slow inhibition in the neocortex. Science 21 (299), 1902–1905.
Traub, R.D., Spruston, N., Soltesz, I., Konnerth, A., Whittington, M.A., Jefferys, G.R., 1998. Gamma-frequency oscillations: a neuronal population phenomenon, regulated by synaptic and intrinsic cellular processes, and inducing synaptic plasticity. Prog. Neurobiol. 55, 563–575.
Veniero D, Bortoletto M, Miniussi C. (2009). TMS-EEG co-registration: On TMS-induced artifact.Clin Neurophysiol. Clin Neurophysiol;120(7):1392-9. Jun 15.
Van Der Werf, Y.D., Paus, T., 2006. The neural response to transcranial magnetic stimulation of the human motor cortex. I. Intracortical and cortico-cortical contributions. Exp. Brain Res. 175 (2), 231–245.
Van Der Werf, Y.D., Sadikot, A.F., Strafella, A.P., Paus, T., 2006. The neural response to transcranial magnetic stimulation of the human motor cortex. II. Thalamocortical contributions. Exp. Brain Res. 175 (2), 246–255.
Ziemann, U., Rothwell, J.C., Ridding, M.C., 1996. Interaction between intracortical inhibition and facilitation in human motor cortex. J. Physiol. 496, 873–881.
Ziemann, U., Tergau, F., Wassermann, E.M., Wischer, S., Hildebrandt, J., Paulus, W., 1998. Demonstration of facilitatory I wave interaction in the human motor cortex by paired transcranial magnetic stimulation. J. Physiol. 511, 181–190.
Ziemann, U., Rothwell, J.C., 2000. I-waves in motor cortex. J. Clin. Neurophysiol. 17 (4), 397–405.
Ziemann, U., 2003. Pharmacology of TMS. Suppl. Clin. Neurophysiol. 56, 226–231 Review.